Decolorization and degradation of Reactive Black 5 dye by photocatalysis: modeling, optimization and kinetic study

Alok Garg, Vikas K. Sangal, Pramod K. Bajpai*

*Department of Chemical Engineering, Thapar University, Patiala, Punjab, India, Tel. +91 175 239 3438; Fax: +91 175 2393005;
emails: alok.garg@thapar.edu (A. Garg), vksangal@gmail.com (V.K. Sangal), pkbajpai@thapar.edu (P.K. Bajpai)*

ABSTRACT

Photocatalytic treatment of Reactive Black 5 dye wastewater was carried out using suspension of commercially available TiO_2 catalyst under ultraviolet irradiation in a shallow pond reactor. An artificial neural network (ANN) model was developed to predict the behavior of the process. Six operational parameters (TiO_2 dose, initial dye concentration, pH of the dye solution, area to volume ratio, UV light intensity, and time) were employed as input and decolorization and degradation efficiencies were employed as output of the network. The outcomes have been validated experimentally indicating that the ANN provided reasonable predictive performance. The parameteric optimization was done, using multiresponse optimization with desirability function approach, to simultaneously maximize the decolorization and degradation efficiency. Optimization by Box–Behnken design effectively copes with interaction between optimizing variables and its prediction agreed well with the results of ANN model and experimental run. The decolorization and degradation follows the pseudo-first-order kinetics.

Keywords: Photocatalysis; Reactive Black 5 (RB5); Textile dyeing wastewater; Decolorization; Degradation efficiency; Modeling; Optimization

1. Introduction

Azo dyes are a significant class of artificial, colored, and organic compounds. Generally, one or more azo bonds (–N=N–) are present in azo dyes. The use of azo dyes is more than 50% of the total dyeing in the textile industry, even though important amounts are consumed for coloring of materials such as leather, paper, plastics, petroleum products, and food [1]. It has been estimated that 1–15% of the dye concentration is lost during the dyeing processes and released as wastewater [2]. The release of the dye wastewater into the ecosystem, million cubic meters discharged per year to wastewater treatment systems, is a remarkable source of aesthetic pollution, eutrophication, and perturbation in aquatic life. Therefore, the treatment of colored wastewater is necessary before being released to the environmental [3]. It is necessary to find an efficient method to eliminate these dyes from industrial effluents. A number of processes like adsorption on activated carbon (charcoal), precipitation, photocatalysis, photofenton, oxidation, and biological methods have been used for the treatment of dye containing wastewaters [4–10]. Almost all the wastewater treatment processes excluding photocatalysis are either less effective in treating

*Corresponding author.

these contaminated wastes and/or are simply subsequent transfer of noxiousness from waste to huge amount of solid waste [11].

Photocatalysis is a promising technique for the treatment of contaminated waters and ground waters, which has been widely studied in the recent years due to its ability to oxidize organic molecules completely without the accumulation of hazardous byproducts. Many researchers find that for photocatalysts, TiO_2 is the most suitable semiconductor material for industrial applications; recognized for its high efficiency, low-cost, high physical and chemical stability, widespread availability, and non-corrosive property [12].

Photocatalytic degradation of Reactive Black 5 (RB5) depends on general reaction parameters like dye concentration, TiO_2 dose, pH, and reaction time. The maximum rate of decolorization of RB5 was found in acidic medium [13–16]. Neamtu et al. [17] have carried out photocatalytic degradation experiments to degrade non-hydrolyzed reactive dyes (Reactive Red 120, Reactive Black 5, Reactive Yellow 84) using UV/H_2O_2 and found 99.6% decolorization.

A comparison of treatment studies using UV/TiO_2 for wastewater containing dyes is given in Table 1. Unfortunately, most of the works reported in the literature showed the results for the color removal and/or COD removal and did not report any data on the dye degradation. Usually the progress of the photocatalytic reactions is followed only by observing the disappearance of the dye color (decolorization) at its maximum absorption wavelengths. The evidence about actual mineralization (degradation) of the dye needs to be studied. The treatment of textile wastewater by photocatalysis has been shown degradation efficiency in terms of color removal and/or COD removal in open literature. In general, color removal is wrongly taken as dye degradation. If any color removal takes place during the treatment, it is not always true to understand that respective amount of dye or contaminant has been removed from the wastewater. The dye may be existing in wastewater in its original/degraded form, depending on treatment method applied. So, study of both color removal and dye degradation concurrently clarifies the true treatment efficiency.

Although most of the authors considered the effect of various parameters like dye concentration, TiO_2 dose, pH, and reaction time on the treatment efficiency, there is also a need to study the other reaction parameters such as light intensity and geometrical parameters of experimental setup. Only few works have been reported on the identification of intermediates formed during the photocatalytic (UV/TiO_2) treatment of RB5 dye containing wastewater.

Wastewater treatment by applying AOPs is, in general, quite complex. This is caused by the complexity of solving the equations that involve the radiant energy balance, the spatial distribution of the absorbed radiation, mass transfer, and the mechanisms of a photochemical or photocatalytic degradation involving radical species. Since the photocatalytic process depends on several factors and the modeling of these processes involves a multivariate system, it is evident that these problems cannot be solved by simple linear multivariate correlation [22]. It is also necessary to study the interaction of two parameters at a time.

In the last few years, artificial neural networks (ANNs) have come out as an appealing tools for non-linear process modeling, particularly in the situations where the improvement of conventional regression models becomes unfeasible. ANN is a computer-based model that solves system through iterations without requiring earlier information of the relationships of process parameters. It is also capable of dealing with uncertainties, noisy data, and non-linear relationships. There are various advantages of an ANN-based model including: (1) ANN can be buildup exclusively from the historic process input–output data, (2) detailed information of the process phenomenology is needless for the model development [23], (3) a properly trained model possesses an exceptional simplification capability owing to which it can exactly predict outputs for a new input data. Owing to their numerous attractive characteristics, ANNs have been extensively used in chemical engineering applications such as steady state and dynamic process modeling, process identification yield maximization, etc. [22]. Also, the response surface methodology (RSM) is the most appropriate multivariate correlation in analytical optimization. The ANNs modeling and RSM optimization simultaneously has not been studied so far for the photodegradation of RB5.

Based on the review of the literature, the objectives of this study are placed as (i) to develop ANN model for the photocatalytic decolorization and degradation of RB5, (ii) investigate the effect of process parameters (TiO_2 dose, initial dye concentration, pH of the dye solution, area to volume ratio, UV light intensity, and time) for the decolorization and degradation efficiency of RB5, (iii) to propose a method based on relative importance of process parameters, for the optimization of a photocatalytic degradation of RB5 that will be fast and requiring less number of experimental or simulation runs for optimization, (iv) to understand the kinetics of photocatalytic treatment of RB5 and to propose a kinetic model, and (v) identification of potentially available intermediates formed during the photocatalytic degradation of RB5.

Table 1
Literature review on UV/TiO$_2$ photocatalyst for wastewater containing dyes

Sr. no.	Type of substrate	Catalyst type and loading	Reaction conditions	Parameter studied	Decolonization efficiency	Refs.
1	Reactive Black 5	Degussa P25 1.5 g l^{-1}	Initial conc. 100 mg l^{-1} Initial volume: 500 ml Area/volume: 0.1–0.5 cm^2 ml^{-1} UV irradiation: 240 W	Effect of pH, dye conc, catalyst loading UV intensity A/V ratio of reactor	70% reduction in TOC in 12 h	[11]
2	Remazol Brilliant Blue R, Remazol Black B, Reactive Blue 221, Reactive Blue 222	Degussa P25 0.83 g l^{-1}	Initial conc. 50 mg l^{-1} Initial volume: 150 ml Irradiation time: 120 min Area/volume: 0.201cm^2 ml^{-1} UV irradiation: 125 W	Effect of the pH	>80%	[18]
3	Remazol Black 5 Procion Red MX-5B	TiO$_2$ 0.5 g l^{-1}	Initial conc. 5, 10.5, 21.5, 42.5, 63.5, and 120 mmol l^{-1} Initial volume: 750 ml UV irradiation: 125 W	Effect of the initial dye concentration, mineralization (TOC)	70% reduction in TOC	[19]
4	Procion Red MX-5B, Remazol Black 5	TiO$_2$ 0.5 g l^{-1}	Initial conc. 5, 10.5, 21.5, and 42.5 mol l^{-1} Initial volume: 750 ml UV irradiation: 125 W	Effect of the initial dye concentration mineralization (TOC)	TOC reduction 21, 42 and 84 µmol l^{-1}	[20]
5	Reactive Black 5	TiO$_2$ 0.5 g l^{-1}	Initial conc 20–100 mg l^{-1} Oxygen gas flow rate 0.35 l min^{-1} Irradiation time: 60 min	Effect of pH photodegradation and kinetics, mineralization (TOC)	Second-order degradation rate constant (k) = 5.085 mg l^{-1} min^{-1}, 71% of TOC	[21]
6	Reactive Black 5, Reactive Orange 4	TiO$_2$ 0.25–1.5 g l^{-1}	Initial conc. 250–1,500 mg l^{-1} Initial volume: 1,000 ml Irradiation time: 20 min UV irradiation: 20 W	Effect of catalyst concentration, pH, initial dye concentration, kinetic study	In the case of RB5, maximum rate of decolorization was observed in acidic medium at pH 4, 75% dye degraded	[16]

2. Materials and methods

2.1. Materials

C.I. RB5 was procured from Sigma-Aldrich (Germany) and is used without further purification. Degussa P25 (having 80% anatase and 20% rutile), was kindly supplied by Degussa Co. (Frankfurt, Germany). Hydrochloric acid and sodium hydroxide (S. D. Fine Chemicals Limited, India) were used to adjust the pH. In all the experiments, Millipore water was used for preparing the solutions.

2.2. Photocatalytic degradation experiment

In the UV/TiO$_2$ process, irradiation was carried out with 240 W (30 W × 8, UV–C) mercury lamps of Philips make, which were placed above a batch photocatalytic shallow pond reactor. At the surface of the solution, the light intensity was measured by total UV radiometer (Eppley Laboratory, Inc., USA). The pH of the solution was adjusted using dilute solutions of hydrochloric acid and sodium hydroxide when necessary and measured with a pH meter (Hach USA HQ30d with pH gel probe). The UV lamp were switched on to initiate the reaction. During the irradiation, agitation was maintained to keep the solution homogeneous and to increase the mass transfer coefficient and, as a result, the overall dye decomposition rate.

All experiments were sampled at a regular time intervals using a pipette. The decolorization and degradation efficiency were measured in terms of absorbance using spectrophotometer (Perkin Elmer Lambda 35 UV–vis spectrophotometer) at wavelengths 597 and 312 nm, respectively. Reproducibility of results was checked by conducting the same experiments twice and an excellent match (within ± 5%) was obtained between successive experiments. The total organic carbon (TOC) content in solution was determined by TOC analyzer (Schimadzu model TOC-V$_{CPH}$).

In order to identify the various intermediates (formed during the dye oxidation) present in the treated dye wastewater, GC-MS of the treated dye wastewater was conducted. The GC-MS analysis was performed on Perkin Elmer Clarus 500 GC coupled with a Perkin Elmer Clarus 500 mass spectrometer. The GC was fitted with fused silica capillary columns (25 m × 0.20 μm internal diameter) coated with a 5% diphenyl 95% dimethyl polysiloxane. Helium (99.99%) was used as the carrier gas at 1.0 ml min^{-1}. The injector was operating at 250°C. The column oven was initially set at 50°C for 2 min, then increased to 280°C at the rate of 10°C min^{-1}, and held for 4 min. The MS quadruple and the MS source temperatures were set at 150 and 230°C, respectively. Data acquisition was performed in the full scan mode (m/z in the range of 50–550).

2.3. Modeling and optimization

Data accumulated from the experiments were used for the ANN modeling and optimization were done by Box–Behnken Design (BBD) using the simulated data from ANN model.

2.3.1. Artificial neural network

Multilayered feed forward (MLF) is the most popular neural network that can be trained by a back-propagation learning algorithm [24]. They are useful to an extensive variation of chemical engineering and related problems. MLF forward network involves neurons and layers, as shown in Fig. 1.

In the feed-forward neural net, all the neurons of a particular layer are connected to all the neurons of the layer next to it. The input layer of neurons acts as a distributor and the input to this layer is directly transmitted to the hidden layer. The inputs to hidden and output layers are calculated by performing a weighted summation of all the inputs received from the preceding layer. The weighted sum of the inputs is transferred to the hidden neurons, where it is transformed using an activation function. The output of hidden neurons, in turn, acts as inputs to output neurons where it undergoes another transformation. The most widely used transfer function for the input and hidden layers is the sigmoid transfer function.

All ANN calculations were carried out using MATLAB 2010b mathematical software with ANN toolbox for Windows running on a personal computer (Core 2 Duo processor 2.40 GHz). A three-layered network with a tan-sigmoid transfer function with back-propagation algorithm was designed for this study.

2.3.2. BBD and multiresponse optimization

BBD is a spherical, revolving design, and consists of a central point and the middle points of the edge of the cube circumscribed on a sphere. BBD is able to optimize the number of simulations and/or experimental runs required to be carried out and to determine the possible interparametric effects on decolorization and degradation of RB5 dye. To examine a process or system including a response Y, where Y depends on the input factors $x_1, x_2, \ldots x_k$, the relationship between the response and the input process parameters is described as:
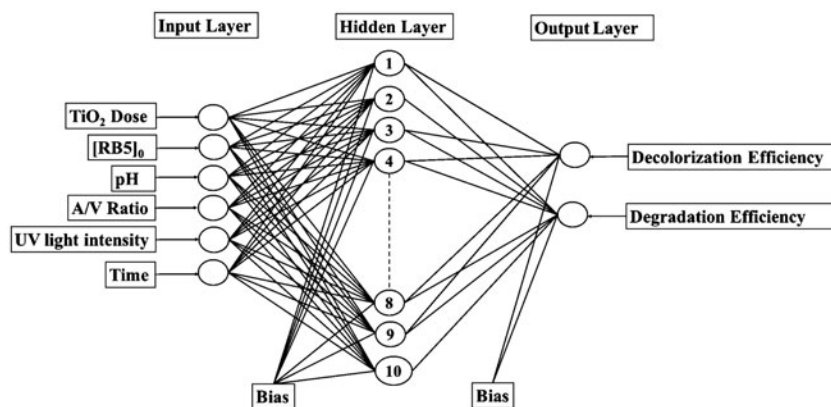
Fig. 1. A schematic view of the developed ANN.

$$Y = h(x_1, x_2, \ldots, x_k) \pm \varepsilon \tag{1}$$

where h is the unknown, but real response function and its format is unknown, and ε is the residual error. A second-order polynomial, Eq. (2), was used through non-linear regression to fit the simulated data and to recognize the relevant model terms. Considering all the linear terms, square terms, and linear-by-linear interaction terms, the quadratic response model can be described as [25]:

$$Y = s_0 + \sum_{i=1}^{k} s_i x_i + \sum_{i=1}^{k} s_{ii} x_i^2 + \sum \sum_{i<j} s_{ij} x_i x_j + \varepsilon \tag{2}$$

where s_0 is the constant, s_i is the slope or linear effect of the input factor x_i, s_{ij} is the linear-by-linear interaction effect among the input factors x_i and x_j, and s_{ii} is the quadratic effect of input factor x_i [26].

There are two responses (decolorization and degradation efficiency) in this study. Therefore, multiresponse process optimization with desirability function approach was used for the optimization of the photocatalysis process parameters. The desirability, d_i, lies between 0 and 1, representing the closeness of a response to its ideal value [25].

The individual desirability functions are combined in order to obtain the overall desirability, D_e, as follows:

$$D_e = (d_1 \times d_2)^{\frac{1}{2}} \tag{3}$$

where d_1 and d_2 are the indiviual desirability of decolorization and degradation efficiency, respectively and $0 \leq D_e \leq 1$.

The statistical software Design-Expert version 6.0.6 (Stat–Ease Inc., Minneapolis, USA) was used for the optimization of the simulated data. For BBD, data have been generated through ANN model. A total of 54 simulation runs have been performed for the optimization by BBD.

3. Results and discussion

3.1. UV−visible analysis

Photodegradation before and during treatment (at various treatment times) was studied using UV−visible analysis (200−800 nm). The spectrum of RB5 in the visible and UV region exhibits a main band with a maximum wavelengths ($\lambda_{\max}$) at 597 and 312 nm in visible and UV region, respectively, as shown in Fig. 2. It has been observed from Fig. 2 that the maximum wavelength peaks are not shifting after degradation of dye till 90 min.

3.2. ANN model development

A three-layered feed forward back propagation neural network (6:10:2) has been used for the modeling of photocatalytic decolorization and degradation of RB5. The range of studied input and output variables has been shown in Table 2.

Optimization of ANN topology is the most important step in the development of a model. To optimize the number of hidden nodes in a layer, a series of topologies were used, in which the numbers of nodes were changed from 2 to 12. Each topology had been repeated two times to remove arbitrary connection due to arbitrary initialization. Mean square error (MSE) was taken as error variable. From Fig. 3, it is

clear that, the MSE is minimum with eight neurons for both (decolorization and degradation efficiency) cases, i.e. the optimized neurons for the process were eight.

In the present work, the training-and-test method was used to weigh the ANN with the trainscg (Scaled conjugate gradient) training function. From the number of experimental data points, 125 data-sets were used to feed the ANN structure. The data-sets were divided into training, validation and test subsets, each of them confined 89, 18, and 18 sets, respectively. The validation and test sets were arbitrarily selected from the experimental data. Fig. 1 shows the schematic diagram of ANN architecture, in which, the input layer has six neurons (TiO$_2$ dose, RB5 concentration, pH, area to volume ratio, UV light intensity, and time) and output layer has two neurons (decolorization and degradation efficiency).

Fig. 4 shows a comparison between simulated and experimental values of the output variable for data-set using neural network model. The correlation coefficients for decolorization and degradation efficiency are 0.9864 and 0.983, respectively. It indicates the reliability of the model and confirmed that the neural network model reproduces both the output responses, decolorization, and degradation efficiency for this system, within experimental ranges adopted for fitting the model.

3.3. Statistical analysis with BBD

A three-level BBD was applied to investigate the photocatalysis process parameters affecting

Table 2
Model variables and their ranges

Variables	Range
Input layer	
TiO$_2$ dose (g l^{-1})	1.0–2.25
RB5 concentration (mg l^{-1})	25–150
pH	2–10
A/V ratio (cm^{-1})	0.112–0.262
UV light intensity (Wm^{-2})	9.4–12.4
Time (min)	0–180
Output layer	
Decolorization efficiency	0–1
Degradation efficiency	0–1
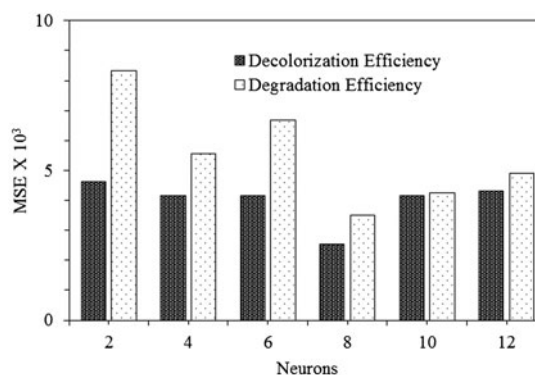
Fig. 3. Effect of the number of neurons in hidden layer.

decolorization and degradation efficiency. A range of values of the TiO$_2$ amount, initial dye concentration, pH of the dye solution, area to volume ratio, light intensity, and time were used as the variable input parameters for the optimization. The input parameters used in the present work are given in Table 3. The factor levels were coded as −1 (low), 0 (central point or middle), and 1 (high) [27].

The simulated data were analysed by regression analysis to fit the equations developed and also for the evaluation of the statistical significance of the equations. The results of the decolorization and degradation efficiency (responses) for photocatalytic degradation of RB5 were analysed according to the design matrix as suggested by BBD.

The sequential *F*-test and other adequacy measures are generally used for selecting the best model. A manual regression method was used to fit the second-order polynomial Eq. (2) to the simulated data and to identify the relevant model terms.

The model summary statistic showed the regression coefficient (R^2) to be the highest for the quadratic

Fig. 2. UV–vis spectral changes of RB5 (50 mg l^{-1}) in aqueous TiO$_2$ dispersion (TiO$_2$ = 1 g l^{-1}) irradiated with a mercury lamp light at neutral pH, after time (1) 0 min, (2) 30 min, (3) 60 min, and (4) 90 min.
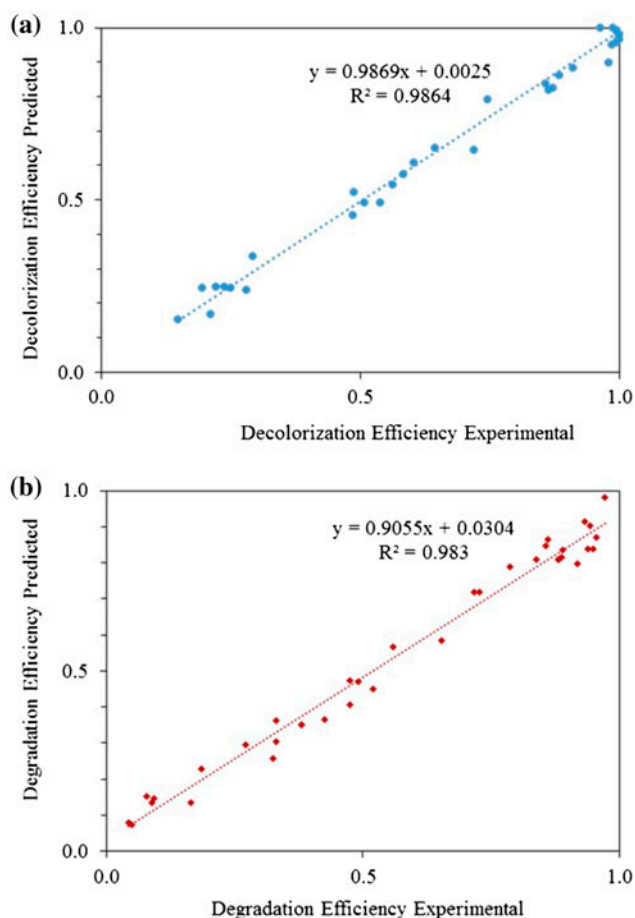
Fig. 4. Comparison of the experimental results with those calculated via neural network modeling for the test set (a) for decolorization efficiency and (b) for degradation efficiency.

model for both the decolorization ($R^2 = 0.9465$) and degradation efficiency ($R^2 = 0.9369$). For the decolorization and degradation efficiency adequate precision ratio were 18.43 and 17.99, respectively. An adequate precision ratio above 4 indicates adequate model efficacy and that the model can be used to navigate the design space [28]. Table 4 shows the analysis of variance (ANOVA) results for the decolorization and degradation efficiency, with a model F-value of 17.03 and 14.29, for decolorization and degradation efficiency, respectively, implying that the model is significant. By eliminating the insignificant model terms, the resulting ANOVA for the reduced quadratic model summarizes the results for each response and shows the significant model terms. TiO$_2$ concentration, initial dye concentration, pH, and time are the highly significant parameters for both decolorization and degradation of RB5. Sahoo and Gupta [29] also reported that initial dye concentration and pH were

the most significant parameters for the photocatalytic degradation of Methylene Blue.

The data points on normal probability plot and a dot diagram of these residuals lie reasonably close to a straight line. This means that the assumptions used in the analysis are satisfied. Therefore, the developed models can be considered to be adequate because the residuals for the prediction of each response are minimum.

The three-dimensional response surface plots of two independent variables, while keeping the other constant, can give information about the individual and interaction effects of the independent variables on the responses. Fig. 5 shows the 3D response surface plots for photocatalytic decolorization and degradation of RB5.

From Fig. 5(a) and (e), it is clear that the maximum decolorization and degradation was in the pH range of 2–4. Also, the decolorization rate and degradation rate increase rapidly with irradiation time. Similar observations were reported by Sahoo and Gupta [29]. The decolorization and degradation efficiency increases with the increase in A/V ratio of the reactor (Fig. 5(b) and (f)).

There is rapid increase in decolorization and degradation efficiency up to 135 min, irrespective of the initial dye concentration (Fig. 5(c) and (g)), after that there is no sharp increase in decolorization and degradation efficiency. Also, the maximum decolorization and degradation was achieved in the concentration range of 25–100 mg l^{-1}.

The point prediction option in the software was used for the optimization of the process parameters. The adequacy of the developed models was verified by carrying out the confirmatory simulation runs using test conditions within the simulation ranges defined earlier. The optimized process parameters at an initial dye concentration of 100 mg l^{-1} are given in Table 5. Table 6 shows the comparisons of decolorization and degradation efficiency obtained by BBD, ANN model, and experimental run at optimum process parameters. Form Table 6, it is clear that, the optimization of process parameters for the photocatalytic degradation of RB5 can be carried out easily and satisfactorily using this method. This method also reduces the number of simulation runs significantly in comparison to other methods reported in literature.

3.4. Adsorption studies of RB5

It is necessary to investigate the adsorption of dye on photocatalyst surface to identify whether the degradation and decolorization of dye has been carried out by photocatalysis or adsorption. The

Table 3
Simulated design levels of chosen variables

| Variables | Levels in Box–Behnken design | | |
	Low (−1)	Medium (0)	High (+1)
TiO$_2$ amount (g l^{-1})	1.00	1.625	2.25
Initial dye conc (mg l^{-1})	25	112.5	200
pH	2	6	10
Area to volume (A/V) ratio (cm^{-1})	0.11	0.185	0.26
Light intensity (Wm^{-2})	8.70	10.35	12
Time (min)	0	90	180

Table 4
ANOVA regression model for RB5 decolorization and degradation efficiency

| Source | Decolorization efficiency | | | | | Degradation efficiency | | | | |
	Sum of squares	DF	Mean square	F-value	Prob. > F	Sum of squares	DF	Mean square	F-value	Prob. > F
Model	6.09	27	0.22	17.03	<0.0001	5.57	27	0.20	14.29	<0.0001
TiO$_2$ amount	0.20	1	0.20	15.49	0.0006	0.11	1	0.11	8.03	0.0087
Initial dye concentration	2.71	1	2.71	204.8	<0.0001	2.58	1	2.58	178.92	<0.0001
pH	0.31	1	0.31	23.47	<0.0001	0.33	1	0.33	23.29	<0.0001
Area to volume ratio	0.032	1	0.032	2.427	0.1313	0.10	1	0.10	7.33	0.0118
Light intensity	0.00	1	0.00	0.05	0.8212	0.01	1	0.01	1.31	0.2620
Time	2.06	1	2.06	156.03	<0.0001	1.55	1	1.55	107.27	<0.0001
(TiO$_2$ amount)^2	0.00	1	0.00	0.05	0.8174	0.00	1	0.00	0.03	0.8434
(Initial dye concentration)^2	0.00	1	0.00	0.47	0.4959	0.14	1	0.14	9.80	0.0043
(pH)^2	0.00	1	0.00	0.35	0.5541	0.00	1	0.00	0.12	0.7273
(Area to volume ratio)^2	0.00	1	0.00	0.00	0.9628	0.00	1	0.00	0.52	0.4749
(Light intensity)^2	0.00	1	0.00	0.05	0.8203	0.00	1	0.00	0.21	0.6480
(Time)^2	0.08	1	0.08	6.78	0.0150	0.07	1	0.07	4.91	0.0356
(TiO$_2$ amount × initial dye concentration)	0.00	1	0.00	0.00	0.9657	0.00	1	0.00	0.40	0.5308
(TiO$_2$ amount × pH)	0.00	1	0.00	0.34	0.5599	0.00	1	0.00	0.21	0.6456
(TiO$_2$ amount × area to volume ratio)	0.04	1	0.04	3.22	0.0843	0.01	1	0.01	1.07	0.3104
(TiO$_2$ amount × light intensity)	0.00	1	0.00	0.68	0.4148	0.00	1	0.00	0.10	0.7437
(TiO$_2$ amount × time)	0.01	1	0.01	1.49	0.2321	0.03	1	0.03	2.75	0.1092
(Initial dye concentration × pH)	0.02	1	0.02	1.65	0.2090	0.01	1	0.01	1.00	0.3247
(Initial dye concentration × area to volume ratio)	0.00	1	0.00	0.44	0.5112	0.00	1	0.00	0.23	0.6328
(Initial dye concentration × light intensity)	0.06	1	0.06	5.22	0.0306	0.02	1	0.02	1.88	0.1817
(Initial dye concentration × time)	0.08	1	0.08	6.27	0.0189	0.12	1	0.12	8.49	0.0072
(pH × area to volume ratio)	0.00	1	0.00	0.02	0.8646	0.00	1	0.00	0.01	0.9026
(pH × light intensity)	0.01	1	0.01	1.35	0.2558	0.00	1	0.00	0.57	0.4545
(pH × time)	0.23	1	0.23	17.755	0.0003	0.23	1	0.23	15.92	0.0005
(Area to volume ratio × light intensity)	0.00	1	0.00	0.03	0.8577	0.00	1	0.00	0.00	0.9877
(Area to volume ratio × time)	0.00	1	0.00	0.50	0.4857	0.01	1	0.01	1.11	0.3012
(Light intensity × time)	0.08	1	0.08	6.62	0.0161	0.08	1	0.08	5.65	0.0251
Residual	0.34	26	0.01	–	–	0.37	26	0.01	–	–
Lack of fit	0.34	21	0.01	–	–	0.37	21	0.01	–	–
Pure error	0	5	0	–	–	0	5	0	–	–
Cor total	6.43	53	–	–	–	5.95	53	–	–	–
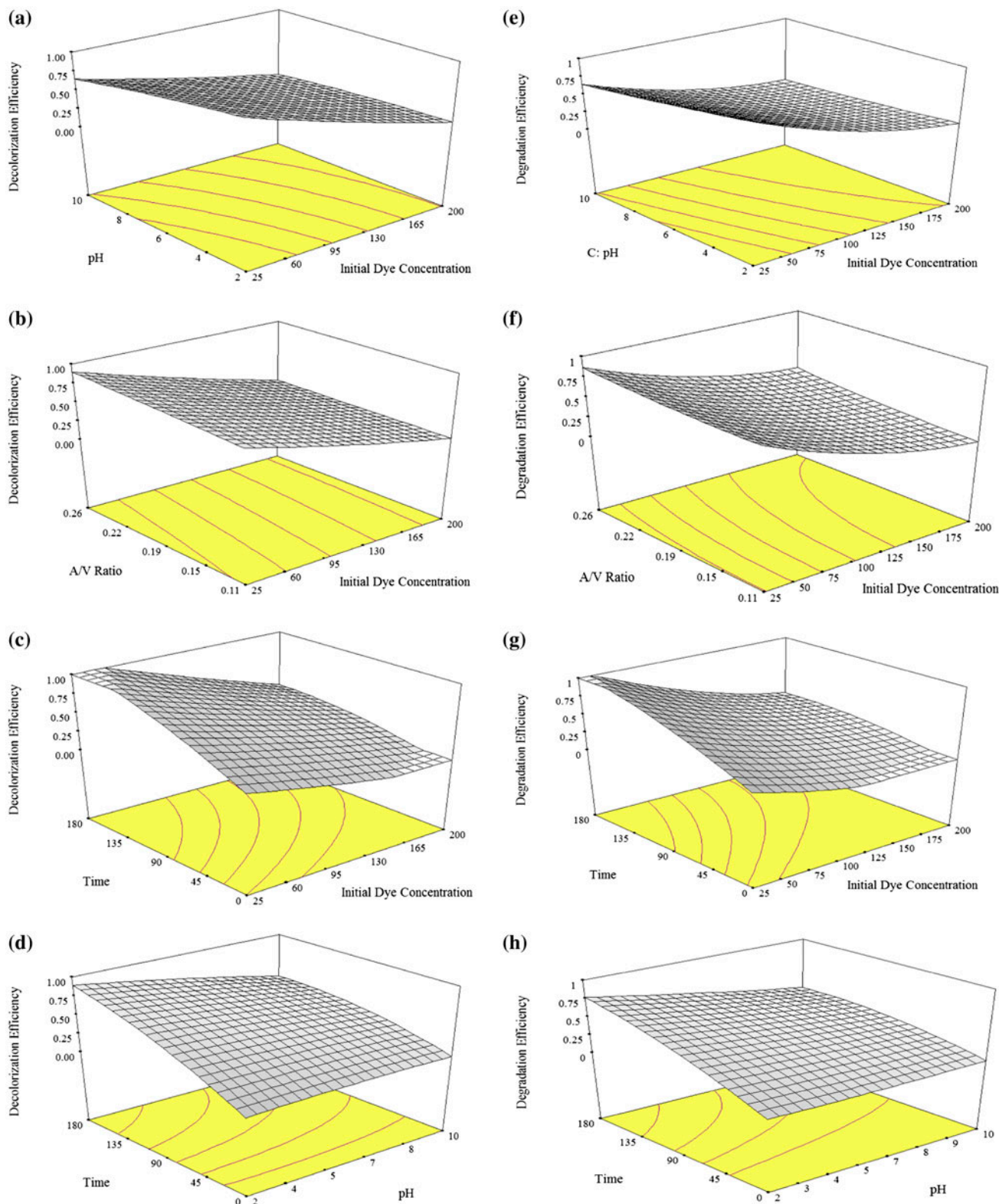
Fig. 5. 3D response surface plots (a) pH Vs initial dye concentration for the decolorization efficiency, (b) A/V ratio vs. initial dye concentration for the decolorization efficiency, (c) time vs. initial dye concentration for the decolorization efficiency, (d) time vs. pH for the decolorization efficiency, (e) pH vs. initial dye concentration for the degradation efficiency, (f) A/V ratio vs. initial dye concentration for the degradation efficiency, (g) time vs. initial dye concentration for the degradation efficiency, and (h) time vs. pH for the degradation efficiency.

Table 5
Optimized parameters suggested by BBD at 100 mg l^{-1} of initial dye concentration

Process parameters	Optimized results
Input	
TiO$_2$ amount (g l^{-1})	2.0
pH	4
Area to volume ratio (cm^{-1})	0.26
Light intensity (Wm^{-2})	12
Time (min)	90

Table 6
Comparisons of decolorization and degradation efficiency between results obtained by BBD, ANN model, and experimental run at optimum process parameters

	Decolorization efficiency	Degradation efficiency
Response from BBD	1	1
Response from ANN	0.98	0.984
Response from experiments	0.99	0.965
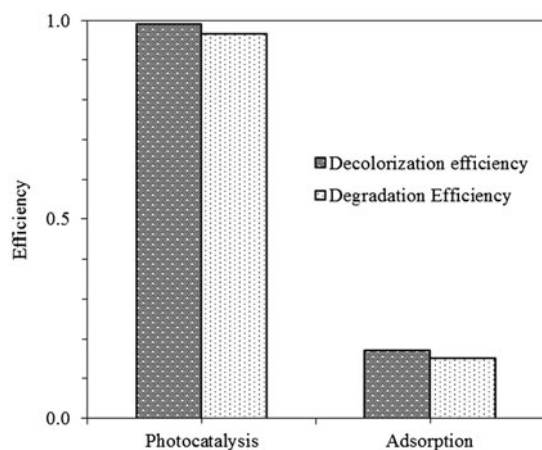
Fig. 6. Comparison between photocatalysis and adsorption.

experiments were carried out under dark conditions using TiO$_2$ to assess the adsorption of RB5 on the surface of photocatalyst which were observed to be 17 and 15% for decolorization and degradation, respectively. UV-induced photocatalytic experiments were conducted using TiO$_2$ catalyst at optimum condition. Fig. 6 shows the comparison between photocatalysis (UV/TiO$_2$) and adsorption (dark/TiO$_2$) of RB5. The decolorization and degradation efficiency of 99 and 96.5% were achieved using TiO$_2$ within 90 min of
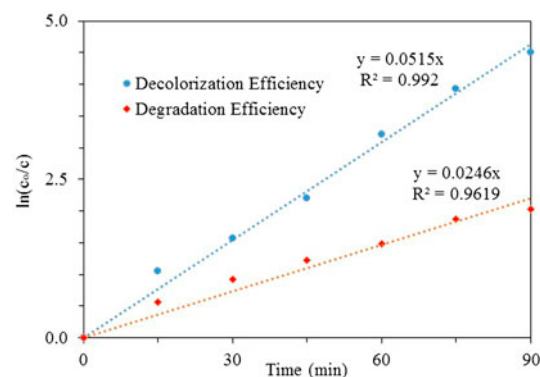
Fig. 7. Reaction kinetics of RB5 at optimized conditions.
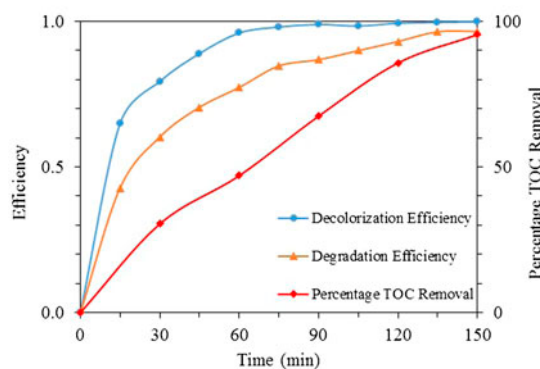
Fig. 8. Variation in the dye decolorization, degradation and TOC removal vs. time at optimized conditions.
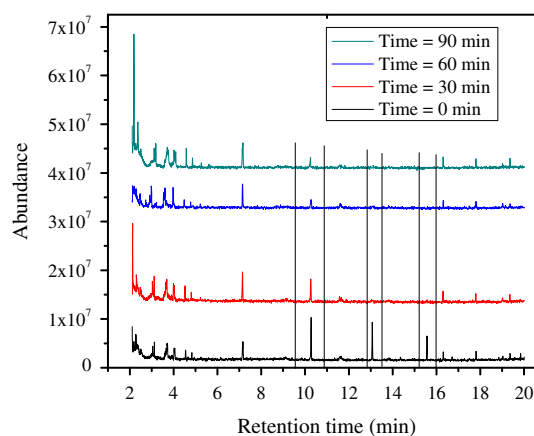
Fig. 9. GC-MS chromatograms of samples.

exposure which illustrates that degradation efficiency achieved was higher in photoinduced catalyzed reactions.

Table 7
Intermediates found by GC-MS

Symbol	Compound	Structural formula	Sample time (min)		
			30	60	90
C_0	Reactive Black 5				
C_1	Ethyl ethanoate		√	X	X
C_2	Urethane		√	X	X
C_3	Hepta-4,6-diyn-2-Ol		√	X	X
C_4	Butanedioic acid 2,3-dihydroxy-dimethyl Ester		√	√	X
C_5	2-(2-sulfanylpropanoylamino) acetic acid		√	√	X
C_6	Propanoic acid, 2-(ethylthio)-ethyl ester		√	√	√
C_7	Tert-Butyl N-hydroxycarbamate		√	√	√
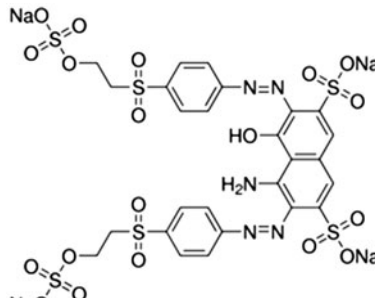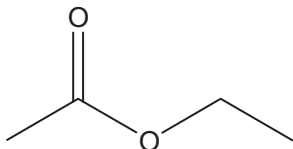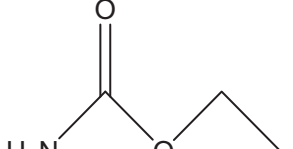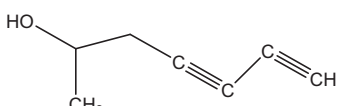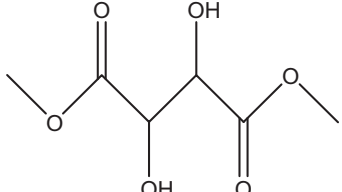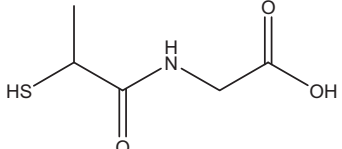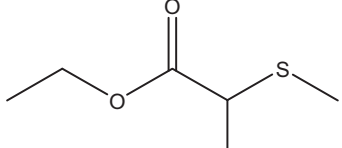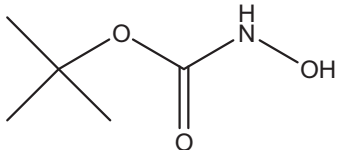
3.5. Kinetic studies

The decolorization and degradation efficiency could be related by a simple power law kinetic model. The pseudo-first-order kinetics in terms of decolorization and degradation efficiency can be written as:

$$\frac{-\mathrm{d}[c]}{\mathrm{d}t} = k'[c] \tag{4}$$

where k' is the pseudo-first-order rate constant.

On integration, (with the limit of $c = c_o$ at $t = 0$) with c_o being the equilibrium concentration of the bulk solution, $\ln c_o/c = k't$, where, c_o is the equilibrium concentration of dye and c is the concentration at time t.

A plot of $\ln c_o/c$ vs. t for photodecolorization and degradation is shown in Fig. 7. A linear relationship between dye concentration and irradiation time has been observed. The kinetic constants are 0.0515 and 0.0246 min^{-1} for decolorization and degradation efficiency, respectively. Barka et al. [30] also found the pseudo-first-order kinetics for photocatalytic degradation of reactive yellow 84.

3.6. TOC removal vs. decolorization and degradation

In order to determine the total degradation during photocatalysis, the TOC, decolorization, and degradation efficiency of RB5 at optimized conditions have been determined and plotted on same curve as shown in Fig. 8. The RB5 dye under optimized conditions shows high decolorization and degradation efficiency and almost completely degraded after 150 min. But TOC removal is slow with respect to degradation efficiency. This will be due to the formation of intermediates and later on these intermediates have been degraded and RB5 mineralized after 150 min.

3.7. Determination of dye degradation products/intermediates in UV/TiO₂ process

GC-MS analysis was carried out to recognize potentially available organic/aromatic compounds/intermediates formed during the photocatalytic degradation of RB5. The photocatalytic degradation was carried out at optimized conditions and samples have been withdrawn at a fixed interval of 30 min. The chromatograms have been shown in Fig. 9 with respect to samples collected at various time intervals like 30, 60, and 90 min of reaction and the chromatogram of original sample (time = 0 min) is also shown. The probable intermediates formed during the photocatalytic degradation of RB5 have been

presented in Table 7. It is clear from Table 7 that after 90 min of irradiation only C_6 and C_7 compounds are left in the dye solution.

4. Conclusions

The present study has demonstrated the use of the ANN modeling and optimization by BBD to determine the parametric values for the decolorization and degradation efficiency for the photocatalytic treatment of RB5. Modeling and optimization results of the photocatalytic treatment of RB5 using ANN and RSM using Design-Expert software are presented and discussed. Multiresponse process optimization using desirability function approach was used to optimize the process parameters. MSE was found to be minimum with eight neurons for both decolorization and degradation efficiency. ANN models have the correlation coefficients of 0.9864 and 0.983 for decolorization and degradation efficiency, respectively, indicating that the ANN model was trained accurately and model can be used to simulate the outputs from a given inputs. It was found that the number of simulation runs reduced significantly for the optimization of photocatalytic treatment of RB5 using BBD. The optimization results of RSM take care of interactions between process variables and the predictions agreed well with the ANN simulation and experimental results.

The optimum conditions for the photocatalytic treatment were estimated for the decolorization and degradation efficiency. The pseudo-first-order kinetics was observed for both decolorization and degradation efficiency. The degradation of RB5 has also been confirmed by removal of TOC at optimum condition.

References

[1] H.A. Abd El-Rehim, E.-S. Ahmed Hegazy, D.A. Diaa, Photo-catalytic degradation of Metanil Yellow dye using TiO₂ immobilized into polyvinyl alcohol/acrylic acid microgels prepared by ionizing radiation, React. Funct. Polym. 72 (2012) 823–831.

[2] Z. Zainal, L.K. Hui, M.Z. Hussein, Y.H. Taufiq-Yap, A.H. Abdullah, I. Ramli, Removal of dyes using immobilized titanium dioxide illuminated by fluorescent lamps, J. Hazard. Mater. 125 (2005) 113–120.

[3] T. Sauer, G. Cesconeto Neto, H.J. José, R.F.P.M. Moreira, Kinetics of photocatalytic degradation of reactive dyes in a TiO₂ slurry reactor, J. Photochem. Photobiol., A 149 (2002) 147–154.

[4] A.R. Khataee, A. Movafeghi, F. Vafaei, S.Y. Salehi Lisar, M. Zarei, Potential of the aquatic fern *Pzolla filiculoides* in biodegradation of an azo dye: Modeling of experimental results by artificial neural networks, Int. J. Phytorem. 15 (2012) 729–742.

[5] M.E. Argun, D. Güclü, M. Karatas, Adsorption of Reactive Blue 114 dye by using a new adsorbent: Pomelo peel, J. Ind. Eng. Chem. 20 (2014) 1079–1084.

[6] M. Karatas, Y.A. Argun, M.E. Argun, Decolorization of anthraquinonic dye, Reactive Blue 114 from synthetic wastewater by Fenton process: Kinetics and thermodynamics, J. Ind. Eng. Chem. 18 (2012) 1058–1062.

[7] M.E. Argun, M. Karatas, Application of Fenton process for decolorization of Reactive Black 5 from synthetic wastewater: Kinetics and thermodynamics, Environ. Prog. Sustain Energy 30 (2011) 540–548.

[8] O. Duman, S. Tunç, T. Gürkan Polat, Adsorptive removal of triarylmethane dye (Basic Red 9) from aqueous solution by sepiolite as effective and low-cost adsorbent, Microporous Mesoporous Mater. 210 (2015) 176–184.

[9] A. Nematollahzadeh, A. Shojaei, M. Karimi, Chemically modified organic/inorganic nanoporous composite particles for the adsorption of Reactive Black 5 from aqueous solution, React. Funct. Polym. 86 (2015) 7–15.

[10] C. Luo, D.L. Wu, Heterogenous Fenton-like oxidation of Reactive Black 5 in water using pyrite cinder, Adv. Mater. Res. 726–731 (2013) 1867–1871.

[11] S.K. Sharma, H. Bhunia, P.K. Bajpai, Photocatalytic decolorization kinetics and mineralization of Reactive Black 5 aqueous solution by UV/TiO$_2$ nanoparticles, Clean Soil Air Water 40 (2012) 1290–1296.

[12] M.A. Barakat, R.I. Al-Hutailah, E. Qayyum, J. Rashid, J.N. Kuhn, Pt nanoparticles/TiO$_2$ for photocatalytic degradation of phenols in wastewater, Environ. Technol. 35 (2013) 137–144.

[13] D. Chatterjee, V.R. Patnam, A. Sikdar, P. Joshi, R. Misra, N.N. Rao, Kinetics of the decoloration of reactive dyes over visible light-irradiated TiO$_2$ semiconductor photocatalyst, J. Hazard. Mater. 156 (2008) 435–441.

[14] O.K. Mahadwad, P.A. Parikh, R.V. Jasra, C. Patil, Photocatalytic degradation of Reactive Black5 dye using TiO$_2$ impregnated ZSM-5, Bull. Mater. Sci. 34 (2011) 551–556.

[15] J. Liu, Z. Zhang, L. Yang, Y. Zhang, S. Deng, The degradation of Reactive Black wastewater by Fe/Cu co-doped TiO$_2$, Int. J. Chem. 3 (2011) 87–92.

[16] S. Kansal, N. Kaur, S. Singh, Photocatalytic degradation of two commercial reactive dyes in aqueous phase using nanophotocatalysts, Nanoscale Res. Lett. 4 (2009) 709–716.

[17] M. Neamtu, I. Siminiceanu, A. Yediler, A. Kettrup, Kinetics of decolorization and mineralization of reactive azo dyes in aqueous solution by the UV/H$_2$O$_2$ oxidation, Dyes Pigm. 53 (2002) 93–99.

[18] C.A.K. Gouvêa, F. Wypych, S.G. Moraes, N. Durán, N. Nagata, P. Peralta-Zamora, Semiconductor-assisted photocatalytic degradation of reactive dyes in aqueous solution, Chemosphere 40 (2000) 433–440.

[19] K. Sahel, N. Perol, H. Chermette, C. Bordes, Z. Derriche, C. Guillard, Photocatalytic decolorization of Remazol Black 5 (RB5) and Procion Red MX-5B—Isotherm of adsorption, kinetic of decolorization and mineralization, Appl. Catal., B 77 (2007) 100–109.

[20] K. Sahel, N. Perol, F. Dappozze, M. Bouhent, Z. Derriche, C. Guillard, Photocatalytic degradation of a mixture of two anionic dyes: Procion Red MX-5B and Remazol Black 5 (RB5), J. Photochem. Photobiol., A 212 (2010) 107–112.

[21] E. Kusvuran, S. Irmak, H.I. Yavuz, A. Samil, O. Erbatur, Comparison of the treatment methods efficiency for decolorization and mineralization of Reactive Black 5 azo dye, J. Hazard. Mater. 119 (2005) 109–116.

[22] A. Aleboyeh, M.B. Kasiri, M.E. Olya, H. Aleboyeh, Prediction of azo dye decolorization by UV/H$_2$O$_2$ using artificial neural networks, Dyes Pigm. 77 (2008) 288–294.

[23] D. Salari, A. Niaei, A. Khataee, M. Zarei, Electrochemical treatment of dye solution containing C.I. Basic Yellow 2 by the peroxi-coagulation method and modeling of experimental results by artificial neural networks, J. Electroanal. Chem. 629 (2009) 117–125.

[24] J. Saien, A.R. Soleymani, H. Bayat, Modeling Fentonic advanced oxidation process decolorization of Direct Red 16 using artificial neural network technique, Desalin. Water Treat. 40 (2012) 174–182.

[25] V.K. Sangal, V. Kumar, I.M. Mishra, Process parametric optimization of a divided wall distillation column, Chem. Eng. Commun. 201 (2013) 72–87.

[26] G.E.P. Box, J.S. Hunter, Multi-factor experimental designs for exploring response surfaces, Ann. Math. Stat. 28 (1957) 195–241.

[27] M. Evans, Optimization of Manufacturing Processes: A Response Surface Approach, Maney Materials Science, London, 2003.

[28] V.K. Sangal, V. Kumar, I.M. Mishra, Optimization of structural and operational variables for the energy efficiency of a divided wall distillation column, Comput. Chem. Eng. 40 (2012) 33–40.

[29] C. Sahoo, A.K. Gupta, Optimization of photocatalytic degradation of methyl blue using silver ion doped titanium dioxide by combination of experimental design and response surface approach, J. Hazard. Mater. 215–216 (2012) 302–310.

[30] N. Barka, S. Qourzal, A. Assabbane, A. Nounah, Y. Ait-Ichou, Photocatalytic degradation of an azo reactive dye, Reactive Yellow 84, in water using an industrial titanium dioxide coated media, Arabian J. Chem. 3 (2010) 279–283.